CONTRACT REPORT ARBRL-CR-00394

# AN IMPROVED NONLINEAR DYNAMIC ANALYSIS OF FLAT LAMINATED PLATES

Prepared by

University of Illinois
Aeronautical and Astronautical
Engineering Department
Urbans, Illinois

March 1979

US ARMY ARMAMENT RESEARCH AND DEVELOPMENT COMMAND
BALLISTIC RESEARCH LABORATORY
ABERDEEN PROVING GROUND, MARYLAND

Destroy this report when it is no longer needed.
Do not return it to the originator.

Secondary distribution of this report by originating or sponsoring activity is prohibited.

Additional copies of this report may be obtained from the National Technical Information Service, U.S. Department of Commerce, Springfield, Virginia 22161.

The findings in this report are not to be construed as an official Department of the Army position, unless so designated by other authorized documents.

*The use of trade names or manufacturers' names in this report does not constitute indorsement of any commercial product.*

UNCLASSIFIED

SECURITY CLASSIFICATION OF THIS PAGE *(When Data Entered)*

| REPORT DOCUMENTATION PAGE | | READ INSTRUCTIONS BEFORE COMPLETING FORM |
|---|---|---|
| 1. REPORT NUMBER<br>CONTRACT REPORT ARBRL-CR-00394 | 2. GOVT ACCESSION NO. | 3. RECIPIENT'S CATALOG NUMBER |
| 4. TITLE *(and Subtitle)*<br>An Improved Nonlinear Dynamic Analysis of Flat Laminated Plates | | 5. TYPE OF REPORT & PERIOD COVERED<br>FINAL 1 Jan 77 - 31 Dec 77<br>6. PERFORMING ORG. REPORT NUMBER |
| 7. AUTHOR(s)<br>Adam R. Zak<br>Daniel W. Pillasch | | 8. CONTRACT OR GRANT NUMBER(s)<br>DAAD05-77-C-0722 |
| 9. PERFORMING ORGANIZATION NAME AND ADDRESS<br>Aeronautical and Astronautical Engineering Dep.<br>University of Illinois<br>Urbans, Illinois | | 10. PROGRAM ELEMENT, PROJECT, TASK AREA & WORK UNIT NUMBERS<br>1LL61102 AH43 |
| 11. CONTROLLING OFFICE NAME AND ADDRESS<br>USA Ballistic Research Laboratory, USA ARRADCOM<br>Aberdeen Proving Ground, MD 21005 (DRDAR-BL) | | 12. REPORT DATE<br>MARCH 1979<br>13. NUMBER OF PAGES<br>31 |
| 14. MONITORING AGENCY NAME & ADDRESS*(if different from Controlling Office)* | | 15. SECURITY CLASS. *(of this report)*<br>Unclassified<br>15a. DECLASSIFICATION/DOWNGRADING SCHEDULE |

16. DISTRIBUTION STATEMENT *(of this Report)*

Approved for public release; distribution unlimited.

17. DISTRIBUTION STATEMENT *(of the abstract entered in Block 20, if different from Report)*

18. SUPPLEMENTARY NOTES

19. KEY WORDS *(Continue on reverse side if necessary and identify by block number)*

Dynamic Analysis
Plate analysis
Finite element
Elastic-visco-plastic
Anisotropic elastic-plastic

20. ABSTRACT *(Continue on reverse side if necessary and identify by block number)*

An improved finite element structural model has been developed for the dynamic analysis of flat laminated plates. This model is an extension of a model which has been developed and reported previously. The original model uses constant thickness quadrilateral elements to represent the shaped of the plate with the elements stacked in thickness direction to account for the material properties of each layer. The new model allows for orthotropic elastic-visco-plastic material response and it uses finite difference equations for the time integration technique. Simplifying approximation allows for the use of large time (continued)

DD FORM 1 JAN 73 1473 EDITION OF 1 NOV 65 IS OBSOLETE

UNCLASSIFIED

SECURITY CLASSIFICATION OF THIS PAGE *(When Data Entered)*

increments in the finite difference equations for time integration.

TABLE OF CONTENTS

# I. INTRODUCTION

The purpose of this investigation has been to improve a finite element program which performs three dimensional analysis for impulsively loaded laminated plates (acronym TIP)[1]. This TIP program has a finite element model that uses the quadrilateral to define the shape of the element in the plane of the plate and then arranges a number of these elements through the thickness to describe the necessary number of material layers. Each layer then has its own material properties. The model is nonlinear since it allows for large plate deflections and for material yield effects. The original program only allowed for isotropic elastic-perfectly plastic solids. The dynamic equations are obtained by lumping the mass of the plate into the nodal points of the finite element model and then solving kinematic equations of motions by use of a finite difference technique. The improvements to the TIP program were to decrease the time that the program ran by use of large time increments in the finite-difference equations and to develop an orthotropic elastic-perfectly plastic analysis which was then further improved to include orthotropic elastic-visco-plastic analysis.

The limitations on the size of the integration time step are a direct result of the finite-element model which treats the plate as a lumped mass system where the individual masses are placed at the nodes. Consequently, as the numerical integration proceeds the masses move relative to each other, and if the integration time step is too large, an artificial oscillation was observed by examining the internal forces acting on each mass for successive time steps. When a relatively large time step is used these forces will change sign for each successive time step. The worst condition occurs in the thickness direction, since the masses will, in general, be separated by a much smaller distance in this direction. In addition to this, it has been observed from previous numerical results that the two inplane displacements vary relatively smoothly through the thickness and therefore, they are modified to vary linearly without restricting any shear deformation.

The orthotropic yield analysis uses the same technique that was used in the original TIP program with only the yield criterion changing. For the orthotropic elastic-perfectly plastic analysis, Hill's Yield Criterion[2] is used instead of von Mises Yield Criterion. Additional orthotropic yield stresses are also needed as additional input. For the elastic-visco-plastic analysis a strain rate dependence is

---

[1] Zak, Adam R., "Nonlinear Dynamic Analysis of Flat Laminated Plates by the Finite Element Method," Final Report, Contract No. DAADO5-73-C-0197, University of Illinois, February, 1977.

[2] Hill, R., "The Mathematical Theory of Plasticity," Clarendon Press, Oxford, 1950.

introduced by use of an extension of the isotropic Bingham material[3] to the orthotropic case.

## II. MODIFICATION FOR LARGE TIME INCREMENTS

### Analysis

In this analysis the in-plane (u and v) displacements are handled separately from the displacements through the thickness (w), but, both utilize the finite difference equation:

$$\begin{aligned}\{\Delta\}_{n+1} &= 2\{\Delta\}_n - \{\Delta\}_{n-1} \\ &+ \beta h^2 [M]^{-1} \left[\{F_I\}_{n+1} + \left(\frac{1}{\beta} - 2\right)\{F_I\}_n + \{F_I\}_{n-1}\right] \\ &+ \beta h^2 [M]^{-1} \left[\{F_E\}_{n+1} + \left(\frac{1}{\beta} - 2\right)\{F_E\}_n + \{F_E\}_{n-1}\right]\end{aligned} \tag{1}$$

where $\{\Delta\}$ is the displacement matrix, $\beta$ is the acceleration parameter, h is the time interval, $\{F_I\}$ is the internal force matrix, $\{F_E\}$ is the external force matrix, [M] is the mass matrix, and the subscripts n, n-1, n+1 denotes time intervals.

In analyzing the u and v displacements, it is assumed that they are linearly dependent through the thickness. This forces plane sections to remain plane.

This first assumption results in the following equations:

$$\begin{aligned}u &= q_1 + zq_2 \\ v &= q_3 + zq_4\end{aligned} \tag{2}$$

where $q_k$, k=1, 4, are unknown coefficients called the transformed displacements and z is the distance in the z-direction of the node from the center of gravity. The importance of having z be the distance from the center of gravity will be discussed when the transformed mass matrix is discussed. In matrix notation equation (2) becomes:

---

[3]Cristescu, No., "Dynamic Plasticity," North Holland Publishing Company, 1967.

$$\{\Delta\} = [TF]\ \{q\} \tag{3}$$

where $\{q\}$ is the matrix of transformed displacements and $[TF]$ is the transformation matrix described below. Letting $\ell$ be the number of layers of material and $i=1, \ell+1$ be the nodal location in the thickness direction, the transformation matrix can be written as:

$$[TF] = \begin{bmatrix} [TF_1] \\ [TF_2] \\ \cdot \\ [TF_i] \\ \cdot \\ [TF_{\ell+1}] \end{bmatrix} \tag{4}$$

where

$$[TF_i] = \begin{bmatrix} 1 & Z_i & 0 & 0 \\ 0 & 0 & 1 & Z_i \end{bmatrix} \tag{5}$$

and $Z_i$ is the distance of node i from the center of gravity. $i=1$ is the node at the bottom of the plate and $i=\ell+1$ is the node at the top.

Since the displacements are written in terms of transformed displacements, then the forces should be written in terms transformed forces. Letting $\{f_E\}$ be the matrix of external forces corresponding to $\{q\}$, and $\{f_I\}$ be internal forces also corresponding to $\{q\}$, the theory of virtual work states:

$$d\{\Delta\}^T\{F_I\} = d\{q\}^T\{f_I\} \tag{6}$$

Transposing equation (3) yields:

$$\{\Delta\}^T = \{q\}^T\ [TF]^T \tag{7}$$

Substituting equation (7) into (6) yields:

$$d\{q\}^T\ [TF]^T\ \{F_I\} = d\{q\}^T\ \{f_I\} \tag{8}$$

Therefore:

$$\{f_I\} = [TF]^T \{F_I\} \tag{9}$$

Similarly:

$$\{f_E\} = [TF]^T \{F_E\} \tag{10}$$

Finding a transformed mass matrix [m] starts with:

$$- [M] \{\ddot{\Delta}\} = \{F\}_{inertia} \tag{11}$$

By virtual work:

$$- d\{\Delta\}^T [M] \{\ddot{\Delta}\} = d\{\Delta\}^T \{F\}_{inertia} \tag{12}$$

$$- d\{q\}^T [m] \{\ddot{q}\} = d\{\Delta\}^T \{F\}_{inertia} \tag{13}$$

$$d\{\Delta\}^T [M] \{\ddot{\Delta}\} = d\{q\}^T [m] \{\ddot{q}\} \tag{14}$$

Substituting equations (3) and (7) into (14) yields:

$$d\{q\}^T [TF]^T [M] [TF] \{\ddot{q}\} = d\{q\}^T [m] \{\ddot{q}\} \tag{15}$$

Dividing out the unnecessary terms gives:

$$[m] = [TF]^T [M] [TF] \tag{16}$$

Now the reason for $Z_i$ being the distance from the center of gravity will become apparent. The calculations are much simplified by the mass matrix being a diagonal matrix as is the case for the original mass matrix. The original mass matrix was:

$$[M] = \{M_j\} \tag{17}$$

where j varies over the total degrees of freedom.

Performing the matrix multiplication in equation (16) using equations (17), (4), and (5) produces

$$[m] = \begin{bmatrix} \sum_{i=1}^{\ell+1} M_i & \sum_{i=1}^{\ell+1} M_i Z_i & 0 & 0 \\ \sum_{i=1}^{\ell+1} M_i Z_i & \sum_{i=1}^{\ell+1} M_i Z_i^2 & \sum_{i=1}^{\ell+1} M_i Z_i & 0 \\ 0 & \sum_{i=1}^{\ell+1} M_i Z_i & \sum_{i=1}^{\ell+1} M_i & \sum_{i=1}^{\ell+1} M_i Z_i \\ 0 & 0 & \sum_{i=1}^{\ell+1} M_i Z_i & \sum_{i=1}^{\ell+1} M_i Z_i^2 \end{bmatrix} \tag{18}$$

But

$$\sum_{i=1}^{\ell+1} M_i Z_i = 0 \tag{19}$$

by definition of the center of gravity, thus causing [m] to be a diagonal matrix.

Referring to equation (1) the only element that still must be transformed is the deflections at past time intervals. From equation (3):

$$\{q\}_n = [TF]^{-1}\{\Delta\}_n \tag{20}$$

Rather than finding the inverse of the entire transformation matrix, it is only necessary to get the inverse of two of the submatrices in equation (4) since it is only necessary to solve for four unknowns. This is easily done by hand and results in:

$$\begin{bmatrix} TF_1 \\ TF_2^1 \end{bmatrix}^{-1} = \begin{bmatrix} 1 - \frac{Z_1}{Z_1-Z_2} & 0 & \frac{Z_1}{Z_1-Z_2} & 0 \\ \frac{1}{Z_1-Z_2} & 0 & -\frac{1}{Z_1-Z_2} & 0 \\ 0 & 1 - \frac{Z_1}{Z_1-Z_2} & 0 & \frac{Z_1}{Z_1-Z_2} \\ 0 & \frac{1}{Z_1-Z_2} & 0 & -\frac{1}{Z_1-Z_2} \end{bmatrix} \quad (21)$$

Substituting the transformed quantities into equation (1) yields:

$$\{q\}_{n+1} = 2\{q\}_n - \{q\}_{n-1} \quad (22)$$

$$+ \beta h^2 [m]^{-1} \left[\{f_I\}_n + \left(\frac{1}{\beta} - 2\right) \{f_I\}_{n-1} + \{f_I\}_{n-2}\right]$$

$$+ \beta h^2 [m]^{-1} \left[\{f_E\}_{n+1} + \left(\frac{1}{\beta} - 2\right) \{f_E\}_n + \{f_E\}_{n-1}\right]$$

It should be noted that the internal transformed forces are displaced by one time increment. Because these forces are small, even at large time increments, this yields accurate results. Equation (22) is thus solved and equation (3) transforms the results to global displacements.

Although this time lag is acceptable for the in-plane displacements, it is not acceptable for the w displacements. The reason for this is the external force is being applied in the w direction, thus making these internal forces more reactive to larger time intervals. In order to account for the change in the internal force a model was sought to couple the deflections through the thickness.

In finding a model to represent what happens through the thickness, it is necessary to see what the unknowns are. From equation (1) the unknowns are $\{\Delta\}_{n+1}$ and $\{F_I\}_{n+1}$. All the other terms are known. In

order to predict what $\{F_I\}_{n+1}$ is, it is necessary to couple the deflections through the thickness and to assume all strains small when compared to the strain in the w-direction. This can be done by letting:

$$\{F_I\}_{n+1} = \{F_I\}_n + \{\Delta F_I\}_{n+1} \tag{23}$$

where $\{\Delta F_I\}_{n+1}$ is the change of the internal force between time intervals. The deflection in the w direction is then coupled by the model shown in Figure 1. This model assumes the stiffness between the nodal points in the thickness direction is much greater than the stiffness between in-plane nodal points. As long as the external force is in the w direction this is a good assumption.

From Figure 1:

$$\Delta F_{I_{i,n+1}} = k_i \left[(\Delta_{i+1,n+1} - \Delta_{i,n+1}) - (\Delta_{i+1,n} - \Delta_{i,n})\right] - k_{i-1} \left[(\Delta_{i,n+1} - \Delta_{i-1,n+1}) - (\Delta_{i,n} - \Delta_{i-1,n})\right] \tag{24}$$

where i refers to the nodal location through the thickness and n refers to the time increment. The predicted stiffness ($k_i$) is gotten from the orthotropic properties ($C_{ij}$, i=1,6, j=1,6). In matrix notation:

$$\begin{Bmatrix} \sigma_x \\ \sigma_y \\ \sigma_z \\ \sigma_{xy} \\ \sigma_{xz} \\ \sigma_{yz} \end{Bmatrix} = \begin{bmatrix} C_{11} & C_{12} & C_{13} & 0 & 0 & 0 \\ C_{21} & C_{22} & C_{23} & 0 & 0 & 0 \\ C_{31} & C_{32} & C_{33} & 0 & 0 & 0 \\ 0 & 0 & 0 & C_{44} & 0 & 0 \\ 0 & 0 & 0 & 0 & C_{55} & 0 \\ 0 & 0 & 0 & 0 & 0 & C_{66} \end{bmatrix} \begin{Bmatrix} \varepsilon_x \\ \varepsilon_y \\ \varepsilon_z \\ \varepsilon_{xy} \\ \varepsilon_{xz} \\ \varepsilon_{yz} \end{Bmatrix} \tag{25}$$

Using the assumption that all strains are small when compared to the strain in the w-direction yields

$$\sigma_z = C_{33}\, \varepsilon_z \tag{26}$$

This gives the stiffness for a unit cube equal to $C_{33}$.
Therefore:

$$k_i = \frac{C_{33_i} \text{Area}_i}{t_i} \tag{27}$$

where $t_i$ is the thickness of layer i, Area i is the area used to compute the mass of the nodal point, and $C_{33i}$ is the orthotropic property of the quadrilateral that the node lies in.
Letting:

$$\begin{aligned} \Delta'_{i,h+1} &= 2\,\Delta_{i,n} + \Delta_{i,n-1} \\ &+ \frac{\beta h^2}{M_i}\left[F_{I_{i,n}} + \left(\frac{1}{\beta} - 2\right) F_{I_{i,n}} + F_{I_{i,n-1}}\right] \\ &+ \frac{\beta h^2}{M_i}\left[F_{E_{i,n+1}} + \left(\frac{1}{\beta} - 2\right) F_{E_{i,n}} + F_{E_{i,n-1}}\right] \end{aligned} \tag{28}$$

and substituting equations (23) and (28) into (1) produces:

$$\begin{aligned} \Delta_{i,n+1} = \Delta'_{i,n+1} + \frac{\beta h^2}{M_i}\Big[ & k_i\left(\Delta_{i+1,n+1} - \Delta_{i,n+1}\right) \\ & - k_{i-1}\left(\Delta_{i,n+1} - \Delta_{i-1,\,n+1}\right) - k_i\left(\Delta_{i+1,n} - \Delta_{i,n}\right) \\ & + k_{i-1}\left(\Delta_{i,n} - \Delta_{i-1,n}\right)\Big] \end{aligned} \tag{29}$$

where the only unknowns are the deflections at time n+1. This produces i=ℓ+1 (ℓ is the number of layers) number of simultaneous equations which can be solved for.

## Numerical Results and Conclusions

The modified computer program was applied to the dynamic plate problem for which BRL experimental data is available, and which was analyzed by the original computer program.

In the original analysis, before the modifications described here were incorporated, the maximum time step which could be used without numerical instability was 0.25 microseconds (μs). In the modified program time step as large as 10 μs was used. Figures 2 to 4 contain some typical results. Figure 2 shows the results for a time step of 2.5 μs and Figure 3 has similar results for 5 μs. Figure 4 contains the results for a variable time step calculation where 1 μs integration interval was used for time from 0 to 10 μs, followed by a time step of 5 μs from 10 μs to 60 μs, and finally 10 μs time step for time of 60 μs to 100 μs. The results show the plate center deflection as a function of time for the bottom and the top of the plate. These results are compared with the results from the HEMP solution and the experimental data which are only given for the bottom of the plate. The different time steps were used in order to compare the effect of these on the accuracy. It can be observed that the results for the time step of 2.5 μs, Figure 2, compare more closely with the experimental data than the results for 5 μs, Figure 3. The results for a variable time step, Figure 4, seem to give even more accurate results and compare quite well with the HEMP calculations and the experimental data. It may be mentioned that the results for large time steps introduce artificial errors due to large distortion of the pressure load and, therefore, the errors may not all be due to numerical integration. However, the main conclusion is that the method has been made quite stable and large integration steps can be used.

## III. ORTHOTROPIC ELASTIC-PERFECTLY PLASTIC YIELD

### Analysis

The orthotropic analysis follows the same idea as in the isotropic analysis, but it uses Hill's yield criterion and needs more input as far as yield stresses are concerned. These yield stresses are in the six orthotropic directions and are referred to as $Y_{ij}$ ($i = 1, 3$ and $j = 1, 3$). Before seeing the yield criterion, the following constants are defined as:

$$\bar{Y}_{11} = \frac{1}{Y_{11}^2} - \frac{1}{Y_{22}^2} - \frac{1}{Y_{33}^2} \tag{30}$$

$$\bar{Y}_{22} = \frac{1}{Y_{22}^2} - \frac{1}{Y_{11}^2} - \frac{1}{Y_{33}^2}$$

$$\bar{Y}_{33} = \frac{1}{Y_{33}^2} - \frac{1}{Y_{11}^2} - \frac{1}{Y_{22}^2}$$

Then the yield criterion can be written as:

$$f(\sigma_{ij}) = \frac{\sigma_{11}^2}{Y_{11}^2} + \frac{\sigma_{22}^2}{Y_{22}^2} + \frac{\sigma_{33}^2}{Y_{33}^2} + \frac{\sigma_{12}^2}{Y_{12}^2} + \frac{\sigma_{13}^2}{Y_{13}^2} + \frac{\sigma_{23}^2}{Y_{23}^2} \tag{31}$$

$$+ \overline{Y}_{11}\sigma_{22}\sigma_{33} + \overline{Y}_{22}\sigma_{11}\sigma_{33} + \overline{Y}_{33}\sigma_{11}\sigma_{22} = 1$$

The total stress at $t_{n+1}$ is:

$$\sigma^T_{ij_{n+1}} = \sigma_{ij_n} + d\sigma^T_{ij_{n+1}} \tag{32}$$

The strain increment is divided into elastic ($\varepsilon^e$) and plastic ($\varepsilon^p$) strain.

$$d\varepsilon_{ij} = d\varepsilon^e_{ij} + d\varepsilon^p_{ij} \tag{33}$$

The flow rule is written in the following manner:

$$d\varepsilon^p_{11} = d\lambda\left(\frac{\sigma_{11}}{Y_{11}^2} + \frac{\overline{Y}_{22}\sigma_{33} + \overline{Y}_{33}\sigma_{22}}{2}\right) = d\lambda T_{11} \tag{34}$$

$$d\varepsilon^p_{22} = d\lambda\left(\frac{\sigma_{22}}{Y_{22}^2} + \frac{\overline{Y}_{11}\sigma_{33} + \overline{Y}_{33}\sigma_{11}}{2}\right) = d\lambda T_{22}$$

$$d\varepsilon^p_{33} = d\lambda\left(\frac{\sigma_{33}}{Y_{33}^2} + \frac{\overline{Y}_{11}\sigma_{22} + \overline{Y}_{22}\sigma_{11}}{2}\right) = d\lambda T_{33}$$

$$d\varepsilon^p_{12} = d\lambda \frac{\sigma_{12}}{Y^2_{12}} = d\lambda T_{12}$$

$$d\varepsilon^p_{13} = d\lambda \frac{\sigma_{13}}{Y^2_{13}} = d\lambda T_{13}$$

$$d\varepsilon^p_{23} = d\lambda \frac{\sigma_{23}}{Y^2_{13}} = d\lambda T_{23}$$

where $T_{ij}$ is defined by Equation (34). This could be written as:

$$d\varepsilon^p_{ij} = d\lambda\, T_{ij} \tag{35}$$

The orthotropic elastic relation used to evaluate the trail stress is:

$$d\sigma^T_{ij} = C_{ijkl}\, d\varepsilon_{kl} \tag{36}$$

This is substituted into Equation (32) and that result is substituted into Equation (31). Similar to the previous analysis if $f(\sigma_{ij}^T) \leq 1$, then $\sigma^T_{ijn+1} = \sigma_{ij_{n+1}}$, but if $f(\sigma_{ij}^T) > 1$ plastic flow has occurred. Inserting Equation (33) into (36) and that result into (32) gives:

$$\sigma_{ij} = \sigma_{ij}^T - C_{ijkl}\, T_{kl}\, d\lambda \tag{37}$$

Letting $\overline{T}_{ij} = C_{ijk\ell}\, T_{k\ell}$, Equation (37) becomes

$$\sigma_{ij} = \sigma_{ij}^T - \overline{T}_{ij}\, d\lambda \tag{38}$$

Substituting Equation (38) into (31) gives:

$$d\lambda = \frac{C}{B + \sqrt{B^2 - AC}} \tag{39}$$

where:

$$A = \frac{\overline{T}_{11}^2}{Y_{11}^2} + \frac{\overline{T}_{22}^2}{Y_{22}^2} + \frac{\overline{T}_{33}^2}{Y_{33}^2} + \frac{\overline{T}_{12}^2}{Y_{12}^2} + \frac{\overline{T}_{13}^2}{Y_{13}^2} + \frac{\overline{T}_{23}^2}{Y_{23}^2} + \overline{Y}_{11}\,\overline{T}_{22}\,\overline{T}_{33} \qquad (40)$$

$$+ \overline{Y}_{22}\overline{T}_{11}\overline{T}_{33} + \overline{Y}_{33}\overline{T}_{11}\overline{T}_{22}$$

$$B = \frac{\overline{T}_{11}\sigma_{11}^{T}}{Y_{11}^2} + \frac{\overline{T}_{22}\sigma_{22}^{T}}{Y_{22}^2} + \frac{\overline{T}_{33}\sigma_{33}^{T}}{Y_{33}^2} + \frac{\overline{T}_{13}\sigma_{13}^{T}}{Y_{13}^2} + \frac{\overline{T}_{12}\sigma_{12}^{T}}{Y_{12}^2} + \frac{\overline{T}_{23}\sigma_{23}^{T}}{Y_{23}^2}$$

$$+ \overline{Y}_{11}\left(\frac{\overline{T}_{22}\sigma_{33}^{T} + \overline{T}_{33}\sigma_{22}^{T}}{2}\right) + \overline{Y}_{22}\left(\frac{\overline{T}_{11}\sigma_{33}^{T} + \overline{T}_{33}\sigma_{11}^{T}}{2}\right)$$

$$+ \overline{Y}_{33}\left(\frac{\overline{T}_{11}\sigma_{22}^{T} + \overline{T}_{22}\sigma_{11}^{T}}{2}\right)$$

$$C = f(\sigma_{ij}^{T}) - 1$$

This $d\lambda$ is substituted into Equation (38) to give the total stress. In all cases this breaks down to the isotropic case when using appropriate yield stress. After programming, the same results were produced for an isotropic example as were produced in the isotropic elastic-plastic analysis.

## IV. VISCO-PLASTIC MODEL

### Analysis

In this analysis it is assumed that the strain is divided into elastic ($d\varepsilon^e$) and visco-plastic ($d\varepsilon^{vp}$) strain.

$$d\varepsilon = d\varepsilon^e + d\varepsilon^{vp} \qquad (41)$$

Using Hill's Flow Rules, Equation (35) is modified to be:

$$d\varepsilon_{ij}^{vp} = d\lambda \, T_{ij} \tag{42}$$

It should be noted that the visco-plastic strain changes satisfy incompressibility condition

$$\sum_{i=1}^{3} d\varepsilon_{ii}^{vp} = 0 \tag{43}$$

The quantities $T_{ij}$ represent six independent quantities and they can be arranged in a matrix form and then can be related to a stress matrix as follows:

$$\{T\} = [B] \{\sigma\} \tag{44}$$

where:

$$[B] = \begin{bmatrix} \frac{1}{Y_{11}^2} & \frac{\bar{Y}_{33}}{2} & \frac{\bar{Y}_{22}}{2} & 0 & 0 & 0 \\ \frac{\bar{Y}_{33}}{2} & \frac{1}{Y_{22}^2} & \frac{\bar{Y}_{11}}{2} & 0 & 0 & 0 \\ \frac{\bar{Y}_{22}}{2} & \frac{\bar{Y}_{11}}{2} & \frac{1}{Y_{33}^2} & 0 & 0 & 0 \\ 0 & 0 & 0 & \frac{1}{Y_{12}^2} & 0 & 0 \\ 0 & 0 & 0 & 0 & \frac{1}{Y_{13}^2} & 0 \\ 0 & 0 & 0 & 0 & 0 & \frac{1}{Y_{23}^2} \end{bmatrix} \tag{45}$$

By comparing the flow rule in equation (42) to an isotropic case it can be noted that the quantities $T_{ij}$ have the same role as the deviatoric stresses and $\varepsilon_{ij}^{vp}$ strains as the deviatoric strains. In fact, it may be noted that equation (42) reduces in the limit to the isotropic case. Consequently, following the procedure developed for isotropic Bingham material, the strain rate dependence is introduced by defining $\{T^F\}$

$$\{T^F\} = \{T\} + \eta \{\dot{\varepsilon}^{vp}\} \tag{46}$$

where $\eta$ represents viscous coefficient, and $\{T\}$ is the quantity which satisfies the yield criterion.

By using Equation (44) we define:

$$\{\sigma^F\} = [B]^{-1} \{T^F\} \tag{47}$$

If no plastic yield has occurred the viscoplastic strain increment is zero. So we begin this analysis with a trial incremental stress where:

$$\{d\sigma^T\} = [C] \{d\varepsilon\} \tag{48}$$

and [C] is the orthotropic relationship between stress and strain. Equation (48) is inserted into Equation (32) and this is inserted into the yield criterion in Equation (31). If yield does not occur, the trial stress is equal to $\sigma^F$. However, if yield does occur then Equations (46) and (47) must be used to calculate $\sigma^F$ as follows: From Equation (41) and (48):

$$\{d\sigma^F\} = [C] \{d\varepsilon\} - [C] \{d\varepsilon^{vp}\} \tag{49}$$

Then as in Equation (32):

$$\{\sigma^F\} = \{\sigma^T\} - [C] \{d\varepsilon^{vp}\} \tag{50}$$

Multiplying Equation (46) by $[B]^{-1}$ and using Equation (47) in (46) one gets:

$$\{\sigma^F\} = \{\sigma\} + \eta [B]^{-1} \{\dot{\varepsilon}^{vp}\} \tag{51}$$

From Equation (50) and (51), when solving for $\{\sigma\}$ one finds:

$$\{\sigma\} = \{\sigma^T\} - [C] \{d\varepsilon^{vp}\} - \eta [B]^{-1} \{\dot{\varepsilon}^{vp}\} \tag{52}$$

By using Equation (42) it is easily shown that:

$$\{\dot{\varepsilon}^{vp}\} = \{\frac{d\varepsilon^{vp}}{dt}\} = \frac{1}{\Delta t} \{d\varepsilon^{vp}\} = \frac{d\lambda}{\Delta t} \{T\} \tag{53}$$

Substituting (42) and (53) into (52) produces:

$$\{\sigma\} = \{\sigma^T\} - d\lambda[C]\{T\} - \frac{\eta d\lambda}{\Delta t}\ [B]^{-1}\ \{T\} \tag{54}$$

Defining another variable $\{\overline{T}\}$:

$$\{\overline{T}\} = [C]\ \{T\} \tag{55}$$

We use the inverse of Equation (44) and Equation (55) in (54) which produces:

$$\{\sigma\} = \{\sigma^T\} - d\lambda\ \left(\{\overline{T}\} + \frac{\eta}{\Delta t}\{\sigma^T\}\right) \tag{56}$$

The question in a dynamic problem always arises as to what value of stress is used for the flow rule. In this formulation the stress used in the flow rule is approximated by the trail stress. A closer approximation can be formed by doing an iterative loop on this equation, but little difference is found in the solution when this is done.

The $\{\sigma\}$ stress formed here in Equation (56) is substituted into the yield condition and $d\lambda$ is solved for.

This gives the relation:

$$Ad\lambda^2 - 2Bd\lambda + C = 0 \tag{57}$$

where letting:

$$T^*_{ij} = \overline{T}^T_{ij} + \frac{\eta}{\Delta t}\sigma^T \tag{58}$$

$$A = \frac{T^{*2}_{11}}{Y^2_{11}} + \frac{T^{*2}_{22}}{Y^2_{22}} + \frac{T^{*2}_{33}}{Y^2_{33}} + \frac{T^{*2}_{12}}{Y^2_{12}} + \frac{T^{*2}_{13}}{Y^2_{13}} + \frac{T^{*2}_{23}}{Y^2_{23}} \tag{59}$$

$$+ \overline{Y}_{22}\ T^*_{11}\ T^*_{33} + \overline{Y}_{11}\ T^*_{22}\ T^*_{33} + \overline{Y}_{33}\ T^*_{11}\ T^*_{22}$$

$$B = \frac{T^*_{11}\,\sigma_{11}{}^T}{Y^2_{11}} + \frac{T^*_{22}\,\sigma_{22}{}^T}{Y^2_{22}} + \frac{T^*_{33}\,\sigma_{33}{}^T}{Y^2_{33}} + \frac{T^*_{12}\,\sigma_{12}{}^T}{Y^2_{12}} + \frac{T^*_{13}\,\sigma_{13}{}^T}{Y^2_{13}} + \frac{T^*_{23}\,\sigma_{23}{}^T}{Y^2_{23}}$$

$$+ \overline{Y}_{11}\left(\frac{T^*_{22}\,\sigma^T_{33} + T^*_{33}\,\sigma^T_{22}}{2}\right) + \overline{Y}_{22}\left(\frac{T^*_{11}\,\sigma^T_{33} + T^*_{33}\,\sigma^T_{11}}{2}\right)$$

$$+ \overline{Y}_{33}\left(\frac{T^*_{22}\,\sigma^T_{11} + T^*_{11}\,\sigma^T_{22}}{2}\right) \tag{60}$$

$$C = f(\sigma^T_{ij}) - 1 \tag{61}$$

where $f = 1$ is the yield function.
Therefore, from Equation (57)

$$d\lambda = \frac{2B \pm \sqrt{(2B)^2 - 4AC}}{2A} \tag{62}$$

Since $d\lambda \to 0$ as $C \to 0$ the minus sign must be used. Multiplying top and bottom by $B + \sqrt{B^2 - AC}$ produces:

$$d\lambda = \frac{C}{B + \sqrt{B^2 - AC}} \tag{63}$$

This value of $d\lambda$ is then substituted into Equation (56). By using Equations (51), (42), and (44)

$$\{\sigma^F\} = \left(1 + \frac{\eta d\lambda}{\Delta t}\right)\{\sigma\} \tag{64}$$

Equation (64) is used in the modified computer program to calculate the actual stress state in finite-elements.

Numerical Example

The example used to check out the changes in the program was a three layer laminated plate[4]. The top and bottom layer was 1020 steel, 1.27 cm and 1.27 cm thick, respectively. The middle layer was 2040 aluminum .635 cm thick. Values for the viscosity for each material were estimated to be:

298.86 pascal-sec

18.73 pascal-sec

The results for this example are given in Table 1. Table 1 compares with the vertical displacement at the center of the plate of both for the original elastic-plastic and the new elastic-visco-plastic models. It can be seen that for short periods of time the viscous effects are small, but for later times the effect is more pronounced. As expected, the effect of viscosity is to stiffen the plate.

The effect of the viscous material properties do not appreciably alter the dynamic response of steel and aluminum materials. However, this conclusion may not be true for other materials, such as for example, composites, which may exhibit larger viscosity.

## V. CONCLUSIONS

By certain modifications to the TIP computer program it has been possible to increase the incremental time step used in the finite difference time integration. However, even with these modifications, the stresses still oscillate in the thickness direction. It is quite feasible that if the oscillations of the stress can be reduced, further increase in time interval will be possible with an appropriate increase in numerical stability.

The inclusion in the analysis and the computer program of the orthotropic yield criterion and the visco-plastic material response has been successfully accomplished. The viscous effects, however, have been found to be small in the case of one numerical example which uses aluminum and steel materials.

---

[4]Majerus, J.N., and Knapp, R.R., "Dynamic Behavior of Multi-Layered Plate Due to an Intense Impulsive Load," Proceedings of the Second International Conference on Mechanical Behavior of Materials, Boston, Mass., August, 1976.

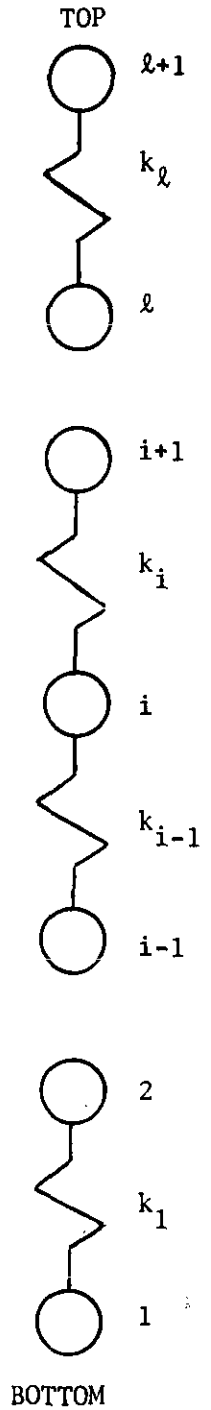


Figure 1. Model representing the predicted stiffness in the thickness direction

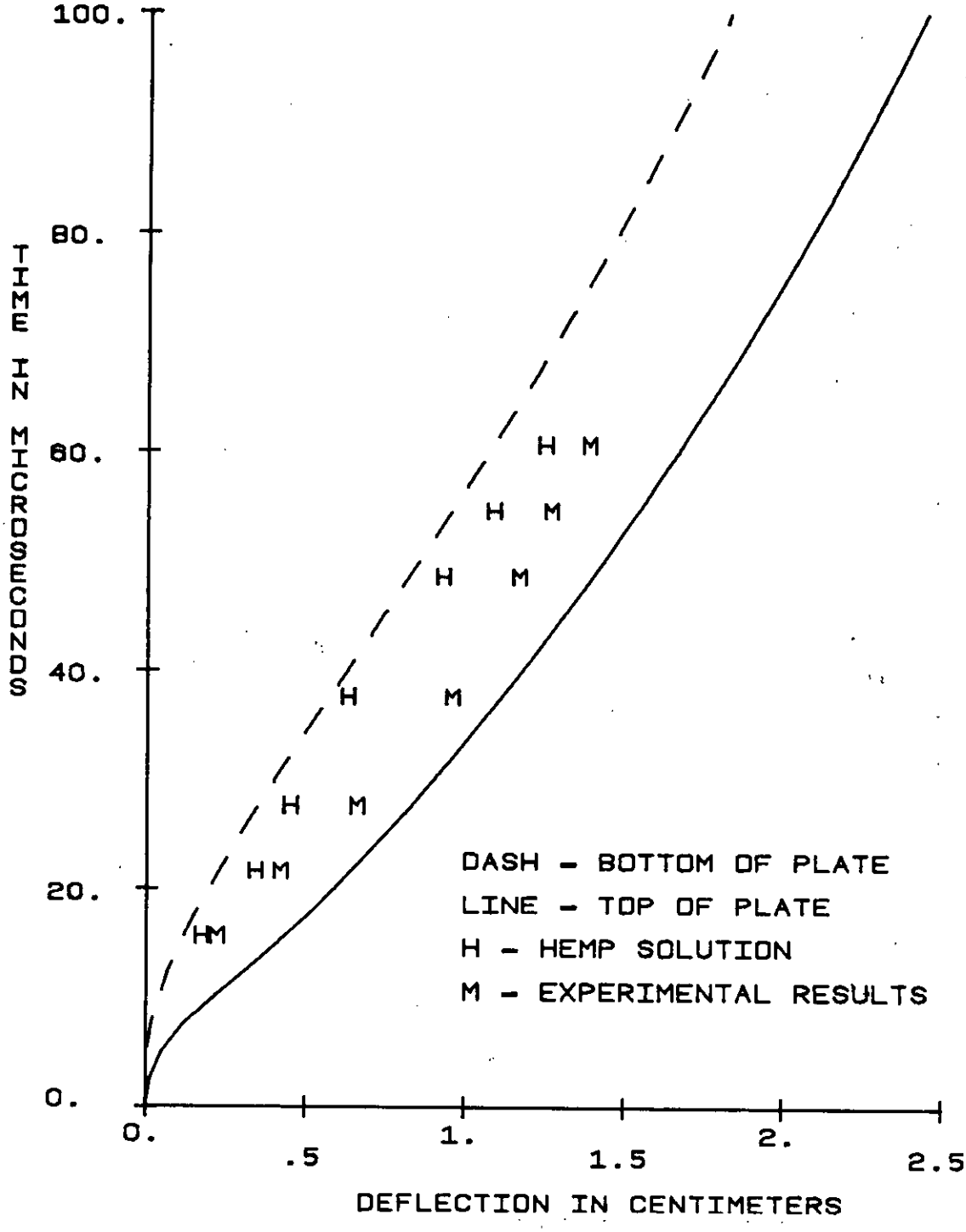


Figure 2. Numerical results for time increment of 2.5 μs

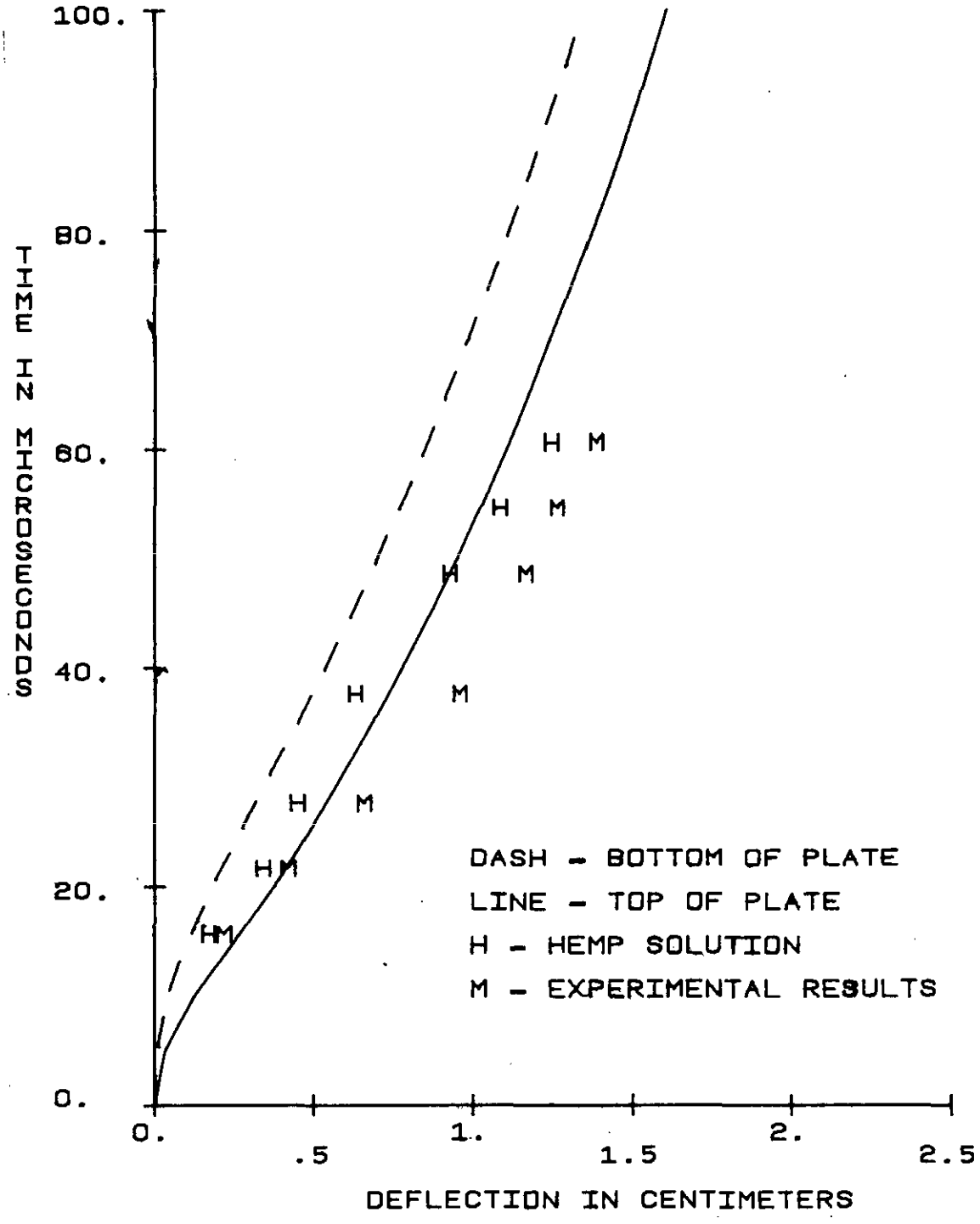


Figure 3. Numerical results for time increment of 5.0 μs

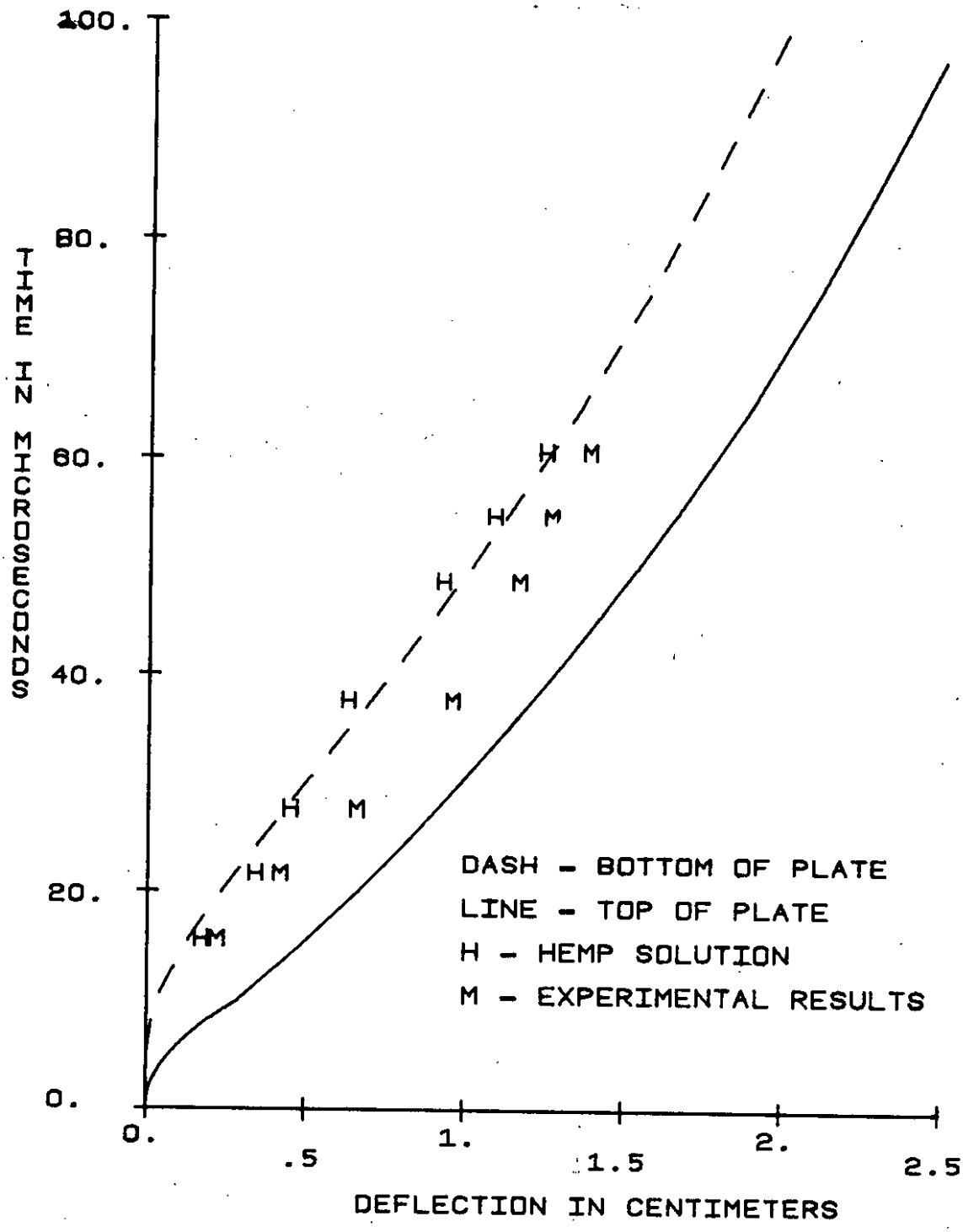


Figure 4. Numerical results for variable time increments of 1.0, 5.0 and 10.0 μs

TABLE 1

Comparison of Results from the Elastic-Plastic and Elastic-Visco-Plastic Models Using Variable Time Steps (see Figure 4)

| Time | Vertical Plate Displacement (cm) for Elastic-Plastic Model | Vertical Plate Displacement (cm) for Elastic-Visco-Plastic Model |
|---|---|---|
| 10 | -.285747 | -.3158007 |
| 20 | -.666216 | -.6348882 |
| 30 | -.9870059 | -.898324 |
| 40 | -1.277305 | -1.1402441 |
| 50 | -1.5436494 | -1.3339216 |
| 65 | -1.9010985 | -1.5438323 |
| 75 | -2.1077580 | -1.6701541 |
| 85 | -2.2934676 | -1.8299201 |
| 95 | -2.4730964 | -1.9608596 |
| 105 | -2.6440384 | -1.9884898 |

DISTRIBUTION LIST

| No. of Copies | Organization |
|---|---|
| 12 | Commander<br>Defense Documentation Center<br>ATTN: DDC-DDA<br>Cameron Station<br>Alexandria, VA 22314 |
| 4 | Director<br>Defense Advanced Research Projects Agency<br>ATTN: Tech Info<br>Dr. E. Blase<br>Mr. T. Bament<br>Dr. G. Sigman<br>1400 Wilson Boulevard<br>Arlington, VA 22209 |
| 1 | Deputy Under Secretary of Defense<br>Tactical Warfare Programs<br>ATTN: Mr. R. Moore<br>The Pentagon, Room 3E1044<br>Washington, DC 20310 |
| 1 | Deputy Under Secretary of Defense<br>Rsch and Advanced Technology<br>ATTN: Mr. R. Thorkildsen<br>The Pentagon, Room 3D1089<br>Washington, DC 20310 |
| 1 | Director<br>Defense Nuclear Agency<br>ATTN: MAJ Spangler<br>Arlington, VA 22209 |
| 1 | Commander<br>US Army Materiel Development and Readiness Command<br>ATTN: DRCDMD-ST, N. Klein<br>5001 Eisenhower Avenue<br>Alexandria, VA 22333 |
| 1 | Commander<br>US Army Aviation Research and Development Command<br>ATTN: DRSAV-E<br>12th and Spruce Streets<br>St. Louis, MO 63166 |
| 1 | Director<br>US Army Air Mobility Research and Development Laboratory<br>Ames Research Center<br>Moffett Field, CA 94035 |
| 1 | Commander<br>US Army Electronics Research and Development Command<br>Technical Support Activity<br>ATTN: DELSD-L<br>Fort Monmouth, NJ 07703 |
| 1 | Commander<br>US Army Communications Rsch and Development Command<br>ATTN: DRDCO-PPA-SA<br>Fort Monmouth, NJ 07703 |
| 2 | Commander<br>US Army Missile Research and Development Command<br>ATTN: DRDMI-R<br>DRDMI-RBL<br>Redstone Arsenal, AL 35809 |
| 1 | Commander<br>US Army Missile Research and Development Command<br>ATTN: DRDMI-YDL<br>Redstone Arsenal, AL 35809 |
| 1 | Commander<br>US Army Tank Automotive Research & Development Cmd<br>ATTN: DRDTA-UL<br>Warren, MI 48090 |

DISTRIBUTION LIST

| No. of Copies | Organization |
|---|---|
| 2 | Commander<br>US Army Armament Research and Development Command<br>ATTN: DRDAR-TSS<br>Dover, NJ 07801 |
| 3 | Commander<br>US Army Armament Research and Development Command<br>ATTN: Mr. E. Barrieres<br>Dr. J. T. Frasier<br>Dr. E. Bloore<br>Dover, NJ 07801 |
| 1 | Commander<br>US Army Armament Materiel and Readiness Command<br>ATTN: DRSAR-LEP-L, Tech Lib<br>Rock Island, IL 61299 |
| 2 | Project Manager<br>Division Air Defense Gun<br>ATTN: DRCPM-ADG, Mr. R. Smith<br>Mr. S. Spaulding<br>Dover, NJ 07801 |
| 6 | Commander<br>US Army Materials and Mechanics Research Center<br>ATTN: DRXMR-T, Mr. J. Bluhm<br>Dr. D. Roulance<br>Dr. A.F. Wilde<br>Dr. J. Mescall<br>DRXMR-ATL<br>Dr. F. Larson<br>Watertown, MA 02172 |
| 1 | Director<br>US Army TRADOC Systems Analysis Activity<br>ATTN: ATAA-SL, Tech Lib<br>White Sands Missile Range<br>NM 88002 |
| 1 | Assistant Secretary of the Army (R&D)<br>ATTN: Asst for Research<br>Washington, DC 20310 |
| 1 | Deputy Assistant Secretary of the Army (R&D)<br>Department of the ARmy<br>Washington, DC 20310 |
| 1 | HQDA (DAMA-ARP)<br>Washington, DC 20310 |
| 1 | HQDA (DAMA-MS)<br>Washington, DC 20310 |
| 1 | Commander<br>US Army Research Office<br>ATTN: Dr. E. Saibel<br>P. O. Box 12211<br>Research Triangle Park<br>NC 27709 |
| 1 | Commander<br>US Army Advanced BMD Technology Center<br>ATTN: BMDATC-M, Mr. P. Boyd<br>P.O. Box 1500<br>Huntsville, AL 35807 |
| 1 | Office of Naval Research<br>ATTN: Code ONR 439, N. Perrone<br>Department of the Navy<br>800 North Quincy Street<br>Arlington, VA 22217 |
| 2 | Chief of Naval Research<br>Department of the Navy<br>ATTN: Code 427<br>Code 470<br>Washington, DC 20325 |

DISTRIBUTION LIST

| No. of Copies | Organization |
|---|---|
| 3 | Commander<br>Naval Air Systems Command<br>ATTN: AIR-604<br>Washington, DC 20360 |
| 2 | Commander<br>Naval Air Systems Command<br>ATTN: Code AIR-310<br>Code AIR-350<br>Washington, DC 20360 |
| 3 | Commander<br>Naval Ordnance Systems Command<br>ATTN: ORD-9132<br>Washington, DC 20360 |
| 1 | Commander<br>Naval Ordnance Systems Command<br>ATTN: Code ORD-0332<br>Washington, DC 20360 |
| 2 | Commander<br>Naval Air Development<br>Center, Johnsville<br>Warminster, PA 18974 |
| 1 | Commander<br>Naval Missile Center<br>Point Mugu, CA 93041 |
| 1 | Commander & Director<br>David W. Taylor Naval Ship<br>Research & Development Ctr<br>Bethesda, MD 20084 |
| 1 | Commander<br>Naval Surface Weapons Center<br>ATTN: Tech Lib, DX-21<br>Dahlgren, VA 22448 |
| 3 | Commander<br>Naval Surface Weapons Center<br>ATTN: Code TX, Dr. W. G. Soper<br>Code G-35<br>W. Elliott<br>W. H. Wishard<br>Dahlgren, VA 22448 |
| 2 | Commander<br>Naval Surface Weapons Center<br>Silver Spring, MD 20910 |
| 1 | Commander<br>Naval Weapons Center<br>ATTN: Code 45, Tech Lib<br>China Lake, CA 93555 |
| 4 | Commander<br>Naval Weapons Center<br>ATTN: Code 4057<br>Code 4011,Dr. E. Lundstrom<br>Code 3813,Mr. M. Backman<br>Code 3835, R.G.S. Sewell<br>China Lake, CA 93555 |
| 2 | Commander<br>Naval Research Laboratory<br>ATTN: Mr. W. J. Ferguson<br>Dr. F. Rosenthal<br>Washington, DC 20375 |
| 1 | Superintendent<br>Naval Postgraduate School<br>ATTN: Dir of Lib<br>Monterey, CA 93940 |
| 1 | USAF (AFRDDA)<br>Washington, DC 20330 |
| 1 | AFSC (SDW)<br>Andrews AFB<br>Washington, DC 20331 |
| 1 | US Air Force Academy<br>ATTN: Code FJS-RL (NC)<br>Tech Lib<br>Colorado Springs, CO 80940 |

DISTRIBUTION LIST

| No. of Copies | Organization |
|---|---|
| 1 | ADTC/DLJW (LTC J. Osborn)<br>Eglin AFB, FL 32542 |
| 1 | AFWL (SUL)<br>Kirtland AFB, NM 87116 |
| 1 | AFAL (AVW)<br>Wright-Patterson AFB, OH 45433 |
| 1 | AFFDL (FDT<br>Wright-Patterson AFB, OH 45433 |
| 1 | AFLC (MMWMC)<br>Wright-Patterson AFB, OH 45433 |
| 1 | AFML/LLN (Dr. T. Nicholas)<br>Wright-Patterson AFB, OH 45433 |
| 2 | ASD (XROT, Gerald Bennett;<br>ENFTV, Martin Lentz)<br>Wright-Patterson AFB, OH 45433 |
| 1 | Headquarters<br>National Aeronautics and<br>Space Administration<br>Washington, DC 20546 |
| 1 | Director<br>National Aeronautics and<br>Space Administration<br>Langley Research Center<br>Langley Station<br>Hampton, VA 23365 |
| 1 | Director<br>National Aeronautics and<br>Space Administration<br>Manned Spacecraft Center<br>ATTN: Lib<br>Houston, TX 77058 |
| 1 | Director<br>Jet Propulsion Laboratory<br>ATTN: LIB (TD)<br>4800 Oak Grove Drive<br>Pasadena, CA 91103 |
| 4 | Director<br>Lawrence Livermore Laboratory<br>ATTN: Mr. M. Wilkins<br>Dr. C. Godfrey<br>Dr. G. Goudreau<br>Dr. R. Werne<br>P. O. Box 808<br>Livermore, CA 94550 |
| 1 | Aeronautical Research<br>Associates of Princeton, Inc.<br>50 Washington Road<br>Princeton, NJ 08540 |
| 1 | AVCO Systems Division<br>ATTN: Dr. W. Reinecke<br>201 Lowell Street<br>Wilmington, MA 01887 |
| 1 | Battelle Columbus Labs<br>ATTN: Mr. J. Backofen<br>505 King Avenue<br>Columbus, OH 43201 |
| 1 | Computer Code Consultants<br>ATTN: Mr. W. Johnson<br>1680 Camino Redondo<br>Los Alamos, NM 87544 |
| 1 | General Electric Company<br>Reentry and Environmental Sys<br>Document Distribution Center<br>ATTN: D. Coceano<br>P. O. Box 7722<br>Philadelphia, PA 19101 |
| 1 | President<br>General Research Corporation<br>ATTN: Lib<br>McLean, VA 22101 |
| 1 | Pacific Technical Corporation<br>ATTN: Dr. F. K. Feldmann<br>460 Ward Drive<br>Santa Barbara, CA 93105 |

DISTRIBUTION LIST

| No. of Copies | Organization |
|---|---|
| 1 | Sandia Laboratories<br>ATTN: Dr. L. Bertholf<br>Albuquerque, NM 87115 |
| 1 | Science Applications, Inc.<br>ATTN: G. Burghart<br>201 W. Dyer Road (Unit B)<br>Santa Ana, CA 92707 |
| 1 | Shock Hydrodynamics<br>ATTN: Dr. L. Zernow<br>4710 Vineland Avenue<br>North Hollywood, CA 91602 |
| 1 | Systems, Science & Software<br>ATTN: Dr. R. Sedgwick<br>P. O. Box 1620<br>La Jolla, CA 92037 |
| 1 | Drexel Institute of Technology<br>Wave Propagation Rsch Center<br>ATTN: Prof. P. Chou<br>32nd & Chestnut Streets<br>Philadelphia, PA 19104 |
| 4 | Southwest Research Institute<br>Dept of Mechanical Sciences<br>ATTN: Dr. U. Lindholm<br>Dr. W. Baker<br>Dr. P. H. Francis<br>A. Wenzel<br>8500 Culebra Road<br>San Antonio, TX 78228 |
| 1 | University of California<br>Los Alamos Scientific Lab<br>ATTN: Dr. R. Karpp<br>P. O. Box 1663<br>Los Alamos, NM 87545 |
| 2 | University of California<br>Los Alamos Scientific Lab<br>ATTN: Dr. J. M. Walsh<br>Tech Lib<br>P. O. Box 1663<br>Los Alamos, NM 87545 |

| No. of Copies | Organization |
|---|---|
| 1 | University of Dayton<br>University of Dayton Research Institute<br>ATTN: Mr. H. F. Swift<br>Dayton, OH 45405 |
| 1 | University of Denver<br>Denver Research Institute<br>ATTN: MR. R. F. Recht<br>2390 S. University Boulevard<br>Denver, CO 80210 |
| 1 | University of Illinois<br>Aeronautical and Astronautical Engineering Department<br>Prof. A. R. Zak<br>Urbana, IL 61801 |

Aberdeen Proving Ground

Dir, USAMSAA
ATTN: Dr. J. Sperrazza
DRXSY-MP, H. Cohen
Cdr, USATECOM
ATTN: DRSTE-SG-H
Dir, Wpns Sys Concepts Team,
Bldg. E3516, EA
ATTN: DRDAR-ACW